

The structure of harvest-induced evolution

1

BIOLOGICAL SCIENCES

2 **Density-dependent selection mediates harvest-induced evolution**

3 Alix Bouffet-Halle¹, Jacques Mériguet^{2,3}, David Carmignac¹, Simon Agostini², Alexis Millot², Samuel
4 Perret^{2,4}, Eric Motard¹, Beatriz Decenciere², Eric Edeline^{1,5*}

5 1: Sorbonne Université, Université Paris Diderot, UPEC, CNRS, INRA, IRD, Institut d'Ecologie et des
6 Sciences de l'Environnement de Paris (iEES-Paris), F-75252 Paris, France.

7 2: CEREEP Ecotron Île-de-France, UMS CNRS ENS 3194, 78 rue du Château, 77140 Saint Pierre-lès-
8 Nemours, France.

9 3: Institut de Biologie de l'Ecole Normale Supérieure, CNRS, INSERM, PSL Research University,
10 Paris, France.

11 4: Centre d'Ecologie Fonctionnelle et Evolutive CEFE, UMR 5175, Campus CNRS, Université de
12 Montpellier, Université Paul-Valéry Montpellier, Montpellier Cedex 5, France.

13 5: INRA, Ecology and Ecosystem Health, 65 rue de Saint-Brieuc, 35042 Rennes Cedex, France.

14 * **Corresponding author:** Eric.Edeline@inra.fr

15 **Key words:** Age and size at maturation, Anthropogenic change, Body size, Fisheries, Harvesting
16 yields, Rapid evolution, Size-dependent selection, *K*-selection, Life-history evolution, Somatic growth
17 rate.

The structure of harvest-induced evolution

18 **Abstract.** Harvesting has been demonstrated to cause rapid, yield-decreasing trait change towards
19 slower somatic growth and earlier maturation in wild populations. These changes are largely
20 considered to result from direct, density-*independent* harvest selection on traits. Here, we show that
21 exact same trait changes may also indirectly result from a harvest-induced relaxation of density-
22 dependent (K) natural selection for faster growth and delayed maturation. We exposed 12 pond
23 populations of medaka fish (*Oryzias latipes*) to contrasted size-selective harvesting during 5 years, and
24 show that harvesting effectively changed juvenile natural mortality from density-dependent to density-
25 independent. We then laboratory-reared medaka progeny under contrasted food levels mimicking the
26 environmental effects of a harvest-induced density gradient. Interaction between past harvest regime
27 and present food environment on progeny traits revealed that harvest-induced trait changes in medaka
28 resulted from selection in a low-food environment only, i.e., were driven by relaxed K -selection only,
29 not by direct harvest selection. Feeding trials further demonstrated that trait changes were associated
30 with reorganizations in rates of food acquisition, assimilation and allocation that were contingent upon
31 the food environments. This is the first study to demonstrate that harvesting can induce undesirable
32 distortions of natural selection that impair productivity traits. We conclude that sustaining harvesting
33 yields over extended time scales requires a preservation of high population densities.

The structure of harvest-induced evolution

34 **Significance statement:** Fisheries management often opposes a density-dependent approach which
35 prioritizes the preservation of high population densities, and an evolutionary approach which considers
36 that alleviating change towards smaller body sizes is paramount to the sustainability of harvesting. The
37 evolutionary approach considers harvest-induced body downsizing to be density-*independent*, i.e., to
38 result only from direct harvest selection against large-bodied individuals. Here, we show instead that
39 harvest-induced body downsizing may be density-dependent because, by decreasing population density,
40 fishing relaxes natural, density-dependent selection for large-bodied individuals. Therefore, preserving
41 population numbers and alleviating body downsizing in harvested populations are not independent lines
42 of management, but are in fact two necessary and complementary routes to reaching the same
43 management objectives.

44

Introduction

45 Harvesting potentially creates a mixture of selective pressures acting in parallel both directly and
46 indirectly on life-history traits. In particular, size-selective harvesting directly selects against an old
47 age, thus favoring early-maturing genotypes, and against large-bodied individuals at a given age, thus
48 favoring slow-growing genotypes (1). This direct, “brute-force” warping of naturally-selected fitness
49 landscapes is currently the prevailing model to explain harvest-induced evolution in wild populations
50 (1–3). However, in parallel harvesting also lowers population densities and is thus susceptible to
51 indirectly warp the naturally-selected fitness landscape through relaxing the strength of density-
52 dependent natural selection (4), also known as *K*-selection (5–7). So far, however, this density-
53 dependent pathway to harvest-induced selection remains unexplored empirically or experimentally. To
54 bridge this gap in our knowledge, we conducted a 5-year size-selective harvesting experiment on 12
55 populations of medaka fish (*Oryzias latipes*) maintained in outdoor ponds under natural conditions with

The structure of harvest-induced evolution

56 no artificial feeding, followed by a 1-generation common garden experiment in the laboratory. The 12
57 founder medaka populations originated from parents wild-caught in Kiyosu (Japan).

58 In ponds, our experimental size-selective fishery removed 81% of the catch (catch rate = 98%) by
59 specifically targeting large-sized individuals (Fig. 1a), and thus successfully reproduced a typical direct
60 harvest selection pattern. In parallel, our experimental fishery relaxed negative density-dependence in
61 medaka populations. Pond medaka populations followed Ricker stock-recruitment dynamics (Fig. 1b),
62 a population dynamics model used in many fisheries management schemes (8). Fishing consistently
63 decreased stock (population size in March) density below ca. 50 individuals (red squares in Fig. 1b), a
64 density region in which increasing stock size had a positive effect on the number of summer-born
65 juveniles (recruitment, black curves, Fig. 1b), indicating demographic “undercompensation” due to
66 density-*in*dependence of vital rates (9). In contrast, unharvested populations had stock sizes above ca.
67 50 individuals (blue triangles in Fig. 1b), a density region where increasing stock size had a negative
68 effect on recruitment, indicating demographic “overcompensation” due negative density-dependence of
69 vital rates (black curves, Fig. 1b).

70 Overcompensating recruitment may operate through decreased fecundity and/or through increased
71 mortality. To discriminate between the two mechanisms, we counted newborn larvae hiding in artificial
72 vegetation in each pond during 3 years. In harvested populations, newborn medaka larvae were on
73 average less numerous than in unharvested populations (P -value = 0.003, Fig. 2, Table S1), but average
74 recruit numbers were similar among unharvested and harvested populations (85 vs. 73 recruits
75 respectively, Fig. 1b, non statistically-significant difference), indicating that overcompensating
76 recruitment was mediated by increased post-larval mortality in medaka populations.

The structure of harvest-induced evolution

77 Density-dependent post-larval mortality is expected to select for a larger body size and delayed
78 reproductive investment. Experiments with *Drosophila* demonstrated that resource competition under a
79 high density favors the evolution of increased food intake and/or conversion efficiency, ultimately
80 resulting in faster somatic growth rates under standardized food conditions (10, 11). In fish,
81 cannibalism is a further source of density-dependent mortality also predicted to favor faster somatic
82 growth to larger body sizes (12, 13). Finally, high density and food limitation are expected to select for
83 a delayed reproduction at a larger body size (6, 14, 15), a prediction that was validated in *Drosophila*
84 (15). Therefore, we predicted that, exactly like direct harvest selection, harvest-induced relaxation of
85 *K*-selection should have favored slower somatic growth rates and earlier maturation in medaka.

86 In a previous laboratory selection experiment, Kiyosu medaka were unable to respond to selection for a
87 smaller body size but were able to respond to selection for a larger body size (16). This previous result
88 suggests that any harvest-induced change in somatic growth or maturation evolved by pond medaka in
89 the present experiment would more likely result from *K*-selection than from direct fishery selection.
90 However, a further, efficient way to discriminate between the direct vs. density-mediated effects of
91 harvesting is through the measurement of interactions between harvest treatments and food levels on
92 trait expression (17–20). This is because the genes that control a given trait are often environment-
93 specific (18–22). Consequently, trait differences measured under different standardized environments
94 may be used to infer the direction of selection in each environment (17, 19, 20).

95 For instance, mice selected for a fast (slow) somatic growth in a high-food environment grow faster
96 (slower) than unselected mice, but only in a high-food environment (18, 19). In contrast, mice selected

The structure of harvest-induced evolution

97 on somatic growth in a low-food environment showed a phenotypic response to selection under both a
98 low- and high-food environments, suggesting that selection on somatic growth in a low-food
99 environment tends to erase the sensitivity of growth to food variation (18–20). Following this rationale,
100 we predicted that somatic growth response to direct, density-*independent* harvest selection in medaka
101 should be manifest in a high-food environment, while somatic growth response to *K*-selection should
102 be manifest in any food environment (19, 20).

103 Evolution of maturation is also expected to be contingent upon the food environment. For instance,
104 predation-induced evolution towards earlier maturation in guppies *Poecilia reticulata* is more
105 pronounced under a high-food environment because predators decrease guppy density and thus select
106 in a high-food environment (17). Hence, we further predicted in medaka that maturation response to
107 direct, density-*independent* harvest selection should be more pronounced in a high-food environment,
108 while maturation response to *K*-selection should be more pronounced under a low-food environment
109 (17).

Results

110
111 To test these predictions we measured in the laboratory the somatic growth of F_1 progeny from pond-
112 sampled parents. We applied a low-, medium- and high-food regimes intended to mimic the
113 environmental effects of an increasing harvest intensity from feeding the progeny once every second
114 day to feeding twice daily.

115 Under all three food environments, harvested medaka grew significantly slower than unharvested
116 medaka (low food P-value = 0.008, medium food P-value < 0.001, high food P-value = 0.002, Fig. 3a).

The structure of harvest-induced evolution

117 Accordingly, a deviance analysis shows that there was no significant harvest by food interaction (P-
118 value = 0.2650, Table 1), indicating that the amplitude of harvest-induced decrease in somatic growth
119 was food-independent. This result suggests that medaka responded to selection for fast-growth in a
120 low-food environment (19, 20), i.e., responded to *K*-selection for faster somatic growth, but not to
121 direct harvest selection for slower somatic growth in a high-food environment. This result is further in
122 line with our previous finding that medaka from Kiyosu are unable to respond to selection for slower
123 somatic growth under laboratory conditions but that they do respond to selection for faster somatic
124 growth (see above).

125 Supporting our second prediction, a deviance analysis shows that the effect of harvesting on the age-
126 dependency of maturation was significantly food-dependent (Age × Harvesting × Food
127 interaction, Table 1). Specifically, harvesting changed the size-corrected effect of age on maturation
128 probability from significantly positive (P-value = 0.025, Table S1) to significantly negative (P-value =
129 0.020, Table S1), reflecting that harvesting induced earlier maturation only in a low-food environment
130 (Fig. 3b). These results suggest that medaka responded to selection for delayed maturation in a low-
131 food environment (17), i.e., responded to *K*-selection, but not to direct harvest selection for earlier
132 maturation in a high-food environment. In line with this result, we previously found that Kiyosu
133 medaka are unable to respond to selection for earlier maturation in the laboratory (16).

134 *K*-selected changes in somatic growth and maturation may be mediated by combined changes in energy
135 acquisition, assimilation or allocation rates. To gain insights into these regulatory pathways we
136 measured acquisition rates through individual feeding trials on laboratory-born F₁ individuals. We

The structure of harvest-induced evolution

137 starved fish overnight, presented them with 20 prey (nauplii of *Artemia salina*), and counted the
138 number of prey eaten during 5 minutes (repeated 3 times per individual).

139 Progeny from harvested populations ate significantly less prey than progeny from unharvested
140 populations, but only in a medium-food environment (P-value = 0.011, Fig. 3c). This result suggest that
141 changes occurred in all three pathways of energy acquisition, assimilation and allocation, but that the
142 respective contributions of these pathways to the expression of life-history change was environment-
143 specific. In a low-food environment, slower somatic growth (Fig. 3a), earlier maturation (Fig. 3b) but
144 unchanged energy acquisition (Fig. 3c, P-value = 0.523) in harvested medaka together suggest energy
145 re-allocation from growth to reproduction. In a medium-food environment, the slower somatic growth
146 (Fig. 3a) of in harvested medaka was apparently mediated by decreased energy acquisition (Fig. 3c),
147 but unchanged maturation (Fig. 3b) also suggests energy re-allocation from growth to reproduction.
148 Finally in a high-food environment, slower somatic growth (Fig. 3a) but unchanged rates of maturation
149 (Fig. 3b) and energy acquisition (Fig. 3c, P-value = 0.424) together suggest decreased energy
150 assimilation rates in harvested medaka. These results are consistent with previous studies showing that
151 evolution towards slower somatic growth in fish may be underlaid by decreases in food consumption
152 rate and conversion efficiency (23).

153

Discussion

154 Our results demonstrate that harvesting caused evolution towards slower somatic growth and earlier
155 maturation in medaka through relaxed K-selection. However, in ponds the body size of 0+ juvenile
156 medaka did not show any statistically significant temporal trend in harvested or unharvested
157 populations (MCMC P-values = 0.365 and 0.262, respectively, Fig. 4). Phenotypic stasis despite known

The structure of harvest-induced evolution

158 evolutionary change (i.e., cryptic evolution) is typical of responses to environmental deterioration
159 where decreased environment quality selects for higher competitive ability but, as highly competitive
160 genotypes spread in the population the environment further deteriorates, resulting in no detectable
161 effects on phenotypes (24, 25). Such cryptic “Red Queen” evolutionary dynamics are expected in all
162 density-dependent populations and are thus probably commonplace in harvested systems. However,
163 their detection requires using common garden experiments or specific quantitative genetic methods (24,
164 25), and studies of harvest-induced trait change based on field data published so far thus maybe
165 underestimate potential for harvest-induced evolution.

166 The direct and density-dependent pathways to harvest-induced selection act in the same direction on
167 life-history traits, but have different implications for management. Phenotypic changes from direct
168 harvest selection may be alleviated by moulding the shape of artificial selection onto the shape of
169 natural selection through, for instance, adjusting gear selectivity. In contrast, the consequences of
170 density-dependent harvest selection can be alleviated only by relaxing the harvest effort (4).
171 Additionally, post-moratorium phenotypic recovery from direct harvest selection is expectedly slow
172 because the strength of natural selection is predicted to be constant and modest relative to the strength
173 of harvest selection. In contrast, recovery from density-dependent harvest selection should be rapid
174 because natural selection strengthens when fishing is relaxed (13).

175 Recent studies have shown that predator-induced life-history evolution may be, at least partly, mediated
176 by relaxed *K*-selection (26) and by an associated adaptation to increased food availability (17). Our
177 study reinforces and extends these previous results by experimentally demonstrating that harvest-
178 induced trait changes previously ascribed to direct, density-independent selection in the literature may,

The structure of harvest-induced evolution

179 in fact, have also emerged through a relaxation of *K*-selection. Hence, the more ecologically sustainable
180 harvesting strategies also produce smaller evolutionary changes (4), and the next-generation harvest
181 management methods should thus converge towards an integration of the reciprocal effects between
182 ecological dynamics and rapid evolutionary change.

183 **Materials and Methods**

184 **Pond medaka populations**

185 *Origin and maintenance*

186 Our start medaka populations descended from 100 wild medaka caught in Kiyosu (27) (Toyohashi,
187 Aichi Prefecture, Japan) in June 2011. These 100 Japanese breeders were maintained in five 20L
188 aquariums and their eggs were collected daily from July to September 2011. Hatched larvae were
189 stocked in 12 circular outdoor ponds (3.57 m diameter, 1.2 m deep).

190 Prior to medaka introduction, the 12 ponds were bottom-coated with a 5 cm layer of Loire River sand,
191 filled with tap water and mildly enriched with a plant fertilizer. After a few weeks of algal
192 development, tanks were seeded with a diverse community of zooplankton collected from surrounding
193 water bodies. Medaka introduction was performed after ponds had reached a clear-water state
194 indicating algal control by zooplankton. After introduction, two pairs of floating plastic brushes were
195 placed in each tank to provide fish with a spawning substrate and shelter for larvae. Each pond was
196 covered with a net to prevent avian predation, and was outlet-secured with a stainless steel filter to
197 prevent any fish or egg escapement. No food was added to the ponds which thus represented natural,
198 replicated ecosystems.

The structure of harvest-induced evolution

199 *Medaka harvesting and phenotyping in ponds*

200 From 2012 to 2016, each of the 12 pond populations was sampled in March before medaka
201 reproduction (pre-recruitment) and in November after medaka reproduction (post-recruitment). Fish
202 were concentrated using a seine net and then fished using handnets (catchability = $98 \pm 0.6\%$ SD
203 estimated using removal sampling). All sampled fish were individually weighted to the nearest mg and
204 estimated for standard body length (from the tip of the snout to the base of the caudal fin) using a body
205 mass-length relationship ($R^2 = 0.98$ on a log-log scale, $n = 2722$). In March in the 6 harvested
206 populations all the fish that were too large to pass through a 2 mm-wide screen were removed, while in
207 unharvested populations all fish were released after phenotyping. In November, all fish from both
208 harvested and unharvested populations were released after phenotyping.

209 *Larvae counts*

210 We visually counted the number of newly-hatched larvae hiding in each pair of floating plastic brushes
211 (summed for the two brush pairs) from one to three times per day at irregular intervals during the 2014,
212 2015 and 2016 spawning periods (April to September).

213 **Medaka F₁ in the laboratory**

214 *Parental fish*

215 In November 2016, between 6 and 10 individuals were randomly kept from each of the 12 pond
216 populations to serve as parents for a F₁ generation in the laboratory. These parental fish were
217 maintained in a greenhouse at air temperature in 12, 150L tanks with live food. In January 2017,
218 parental fish were weighted to the nearest mg, measured for standard body length with ImageJ, and
219 grouped to form 3 breeding pairs per population (except one harvested population that had only one

The structure of harvest-induced evolution

220 female). Each of the resultant 36 pairs was transferred to the laboratory in a 3.5L aquarium and induced
221 to spawn by progressively raising temperature to $27.0 \pm 0.3^{\circ}\text{C}$ and setting a 15-h light:9h dark
222 photoperiod. Dry food (Skretting Gemma Micro) was provided twice per day and live nauplii of
223 *Artemia salina* once per day. After initiation of spawning by all breeding pairs, eggs from each
224 breeding pair were collected daily during a 4-day period, enumerated and incubated in separate jars so
225 as to keep track of individual parental identity (but not spawning day). We found no significant effect
226 of the harvest treatment on parental body size, body condition, fertility or fecundity.

227 *F₁ progeny phenotyping and food environments*

228 We collected F₁ larvae born from the 7th to the 10th day after the weighted average date of spawning.
229 Larvae hatched from the same breeding pair on the same day were transferred to 1.5L aquariums by
230 groups of 3 larvae, and were maintained under the same temperature and light regime as their parents.
231 We kept 1-4 groups of F₁ larvae per breeding pair (average 2.9 groups per breeding pair). At 15 days
232 post hatch (dph), all F₁ individuals were weighted and measured as described above and only one
233 individual per aquarium was randomly kept for subsequent phenotyping, making it possible to track
234 individual developmental trajectories. Individual phenotyping was repeated at 30 dph, 40 dph and then
235 once per week until 90 dph (11 individual measurements). From 40 dph onwards, phenotyping further
236 included detection of the maturity status from the presence of secondary sexual characters (28).
237 Specifically, the maturity criteria were first appearance of a round-shaped anal papilla in females, and
238 of the papillar process on the anal fin in males. Additionally, at around 48, 56 and 63 dph, each
239 individual F₁ medaka was measured for feeding rate. We counted the number of live prey (nauplii of
240 *Artemia salina*) eaten when the medaka was placed alone with 20 prey during 5 minutes in a 80 mL
241 container. Medaka were starved overnight prior to each behavioural test.

The structure of harvest-induced evolution

242 From 15 dph onwards, we varied resource levels by applying three food environments to F₁ progeny.
243 We chose feeding regimes so as to mimic a high-density, scarce-food environment in which predators
244 are not able to daily catch a prey, a low-density, food-rich environment in which predators are replete
245 with prey, and an intermediate environment. In the low-food environment, individuals were fed with
246 2mL of a solution containing nauplii of *Artemia salina* at a standard concentration on day 1, nothing on
247 day 2, dry food (see below) on day 3, nothing on day 4 and so on. In the high-food environment,
248 medaka were fed twice daily, once with nauplii and once with dry food. Finally, in the medium-food
249 environment, medaka were fed once daily alternating nauplii and dry food.

250 Volume of dry food doses and pellet size were increased during fish development to fit with the
251 ontogenetic increase in energy needs and prey size. From 0 to 40 dph, 40 to 60 dph, and 60 dph
252 onwards, medaka received daily 4, 6 and 14 μ L of food, respectively. From 0 to 20 dph, 20 to 40 dph,
253 and 40 dph onwards, dry food was made from 100% 150 μ m pellets, 50% mixture of 150-300 μ m
254 pellets and 100% 300 μ m pellets, respectively.

255 **Statistical analyses**

256 We below provide a short summary of the statistical analyses. A full description is given in the SI
257 Appendix.

258 *Analysis of pond data*

The structure of harvest-induced evolution

259 Medaka age was inferred by fitting a mixture of two Gaussian distributions to individual standard body
260 lengths measurements ($n = 17908$). We further estimated temporal trends in body size of November 0+
261 recruits ($n = 9688$ individuals) using a version of the Gaussian mixture model that was modified to
262 include a harvest treatment-specific ($n = 2$ treatments) hierarchical regression of mean recruit standard
263 body length on year of sampling ($n = 5$ years). We estimated the relationship between individual
264 standard body length and probability to survive through the fishery in March ($n = 3970$ individuals)
265 using a mixed effects Bernoulli GLM with a logit link function. The Gaussian mixture model described
266 above allowed us to estimate the number of November 0+ recruits in each pond and year. We then
267 visualized the strength of negative density-dependence in pond medaka populations by plotting Ricker
268 “stock-recruitment” relationships (Fig. 1b). Finally, larvae counts in ponds were modelled using a
269 mixed-effects zero-inflated negative binomial model, which parameter estimates are provided in Table
270 S1.

271 *Analysis of laboratory data*

272 We estimated the effects of harvesting and food environments on the growth trajectories of F_1 progeny
273 in the laboratory using a second order polynomial regression of standard body length on age (parameter
274 estimates provided in Table S1). We fitted probabilistic maturation reaction norms (PMRNs) to medaka
275 maturation data using the “direct estimation” method for PMRNs (29) in a mixed-effects Bernoulli
276 GLM with a logit link function (parameter estimates provided in Table S1). Counts of the number of
277 nauplii larvae eaten by individual medaka were modelled using a mixed-effects zero-inflated negative
278 binomial model (parameter estimates provided in Table S1).

The structure of harvest-induced evolution

279 **Acknowledgements.** We are grateful to Prof. Kiyoshi Naruse (NIBB, Okazaki, Japan) for his support
280 in obtaining and maintaining wild medaka from Kiyosu.

281 **Funding.** This work has benefited from technical and human resources provided by CEREEP-Ecotron
282 IleDeFrance (CNRS/ENS UMS 3194) as well as financial support from the Regional Council of Ile-de-
283 France under the DIM Program R2DS bearing the references I-05-098/R and 2015-1657. It has
284 received a support under the program "Investissements d'Avenir" launched by the French government
285 and implemented by ANR with the references ANR-10-EQPX-13-01 Planaqua and ANR-11-INBS-
286 0001 AnaEE France, and from Pépinière interdisciplinaire CNRS de site PSL (Paris-Sciences et
287 Lettres) "Eco-Evo-Devo". EE also acknowledges support from the Research Council of Norway
288 (projects EvoSize RCN 251307/F20 and REEF RCN 255601/E40).

289 **Author contributions.** ABH performed the laboratory F_1 experiment, contributed to data analysis,
290 wrote the first draft of the manuscript and contributed to subsequent versions. EE designed the study,
291 contributed to the pond experiment, performed data analysis, and led manuscript writing from the
292 second version. JM, DC, SA, AM, SP, EM and BD contributed to the pond and laboratory experiments.

293 **Competing interests.** The authors declare no competing interests.

294 **Data archiving statement.** All data and codes used in this paper will be archived.

295 **Ethical statement.** The protocols used in this study were designed to minimize discomfort, distress and
296 pain of animals, and were approved by the Darwin Ethical committee (case file #Ce5/2010/041).

297 **Supplementary Materials**

298 Table S1: MCMC parameter estimates for models 4-7.

299 **References**

The structure of harvest-induced evolution

1. Heino M, Díaz Pauli B, Dieckmann U (2015) Fisheries-induced evolution. *Annu Rev Ecol Evol Syst* 46(1):461–480.
2. Edeline E (2016) Life history evolution, human impacts on. *The Encyclopedia of Evolutionary Biology*, ed Kliman R (Academic Press, Oxford), pp 335–342. 1st Ed.
3. Carlson SM, et al. (2007) Four decades of opposing natural and human-induced artificial selection acting on Windermere pike (*Esox lucius*). *Ecol Lett* 10(6):512–521.
4. Engen S, Lande R, Sæther B-E, Associate Editor: Jürgen Groeneveld, Editor: Troy Day (2014) Evolutionary consequences of nonselective harvesting in density-dependent populations. *Am Nat* 184(6):714–726.
5. MacArthur RH, Wilson EO (1967) *The theory of island biogeography* (Princeton University Press, Princeton). 1st Ed.
6. Pianka ER (1970) On r- and K-Selection. *Am Nat* 104(940):592–597.
7. Reznick D, Bryant MJ, Bashey F (2002) r- and K-selection revisited: the role of population regulation in life-history evolution. *Ecology* 83(6):1509–1520.
8. Hilborn R, Walters C (1992) *Quantitative fisheries stock assessment: choice, dynamics and uncertainty* (Springer US). 1st Ed.
9. Bellows TS (1981) The descriptive properties of some models for density dependence. *J Anim Ecol* 50(1):139–156.
10. Mueller LD (1988) Evolution of competitive ability in *Drosophila* by density-dependent natural selection. *Proc Natl Acad Sci U S A* 85(12):4383–4386.
11. Sarangi M, Nagarajan A, Dey S, Bose J, Joshi A (2016) Evolution of increased larval competitive ability in *Drosophila melanogaster* without increased larval feeding rate. *J Genet*:1–13.
12. Claessen D, de Roos AM, Persson L (2000) Dwarfs and giants: cannibalism and competition in size structured populations. *Am Nat* 155(2):219–237.
13. Edeline E, et al. (2007) Trait changes in a harvested population are driven by a dynamic tug-of-war between natural and harvest selection. *Proc Natl Acad Sci* 104(40):15799–15804.
14. Holliday R (1989) Food, reproduction and longevity: is the extended lifespan of calorie-restricted animals an evolutionary adaptation? *BioEssays News Rev Mol Cell Dev Biol* 10(4):125–127.
15. Sgrò CM, Partridge L (2000) Evolutionary responses of the life history of wild caught *Drosophila melanogaster* to two standard methods of laboratory culture. *Am Nat* 156(4):341–353.
16. Renneville C, et al. (2018) Anthropogenic selection along directions of most evolutionary resistance. *bioRxiv*:498683.

The structure of harvest-induced evolution

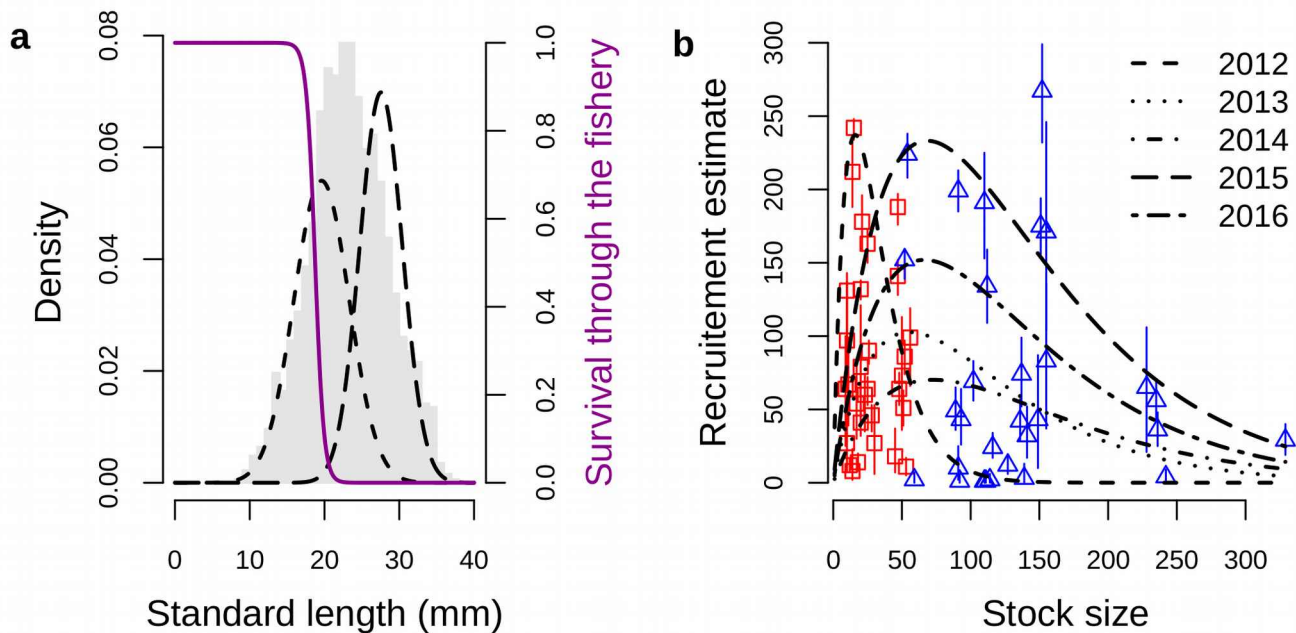
17. Walsh MR, Reznick DN (2008) Interactions between the direct and indirect effects of predators determine life history evolution in a killifish. *Proc Natl Acad Sci* 105(2):594.
18. Falconer DS (1960) Selection of mice for growth on high and low planes of nutrition. *Genet Res* 1(1):91–113.
19. Falconer DS, Latyszewski M (1952) The environment in relation to selection for size in mice. *J Genet* 51(1):67.
20. Falconer DS (1990) Selection in different environments: effects on environmental sensitivity (reaction norm) and on mean performance. *Genet Res* 56(1):57–70.
21. Jinks JL, Connolly V (1973) Selection for specific and general response to environmental differences. *Heredity* 30:33.
22. Falconer DS, Mackay TFC (1996) *Introduction to quantitative genetics* (Longman, Harlow, Essex, UK). 4th Ed.
23. Walsh MR, Munch SB, Chiba S, Conover DO (2006) Maladaptive changes in multiple traits caused by fishing: impediments to population recovery. *Ecol Lett* 9(2):142–148.
24. Wolf JB (2003) Genetic architecture and evolutionary constraint when the environment contains genes. *Proc Natl Acad Sci U S A* 100(8):4655–4660.
25. Hadfield JD, Wilson AJ, Kruuk LEB (2011) Cryptic evolution: does environmental deterioration have a genetic basis? *Genetics* 187(4):1099–1113.
26. Bassar RD, Lopez-Sepulcre A, Reznick DN, Travis J (2013) Experimental evidence for density-dependent regulation and selection on Trinidadian guppy life histories. *Am Nat* 181(1):25–38.
27. Spivakov M, et al. (2014) Genomic and phenotypic characterization of a wild medaka population: towards the establishment of an isogenic population genetic resource in fish. *G3 GenesGenomesGenetics* 4(3):433–445.
28. Yamamoto T (1975) *Medaka (killifish): biology and strains* (Keigaku Pub. Co, Tokyo). 1st Ed.
29. Heino M, Dieckmann U (2008) Detecting fisheries-induced life-history evolution: an overview of the reaction-norm approach. *Bull Mar Sci* 83(1):69–93.
30. Stearns SC, Koella JC (1986) The evolution of phenotypic plasticity in life-history traits: predictions of reaction norms for age and size at maturity. *Evolution* 40(5):893–913.
31. Heino M, Dieckmann U, Godø OR (2002) Measuring probabilistic reaction norms for age and size at maturation. *Evolution* 56(4):669–678.

The structure of harvest-induced evolution

300 **Table 1. Analysis of deviance table for GLMs testing for the harvest by food interaction on life-
301 history traits in laboratory-born F₁ medaka progeny.** The “Deviance” column gives the reduction in
302 the residual deviance as each predictor is added in turn into the model. The P-values compare the
303 reduction in deviance to the residual deviance in an F test.

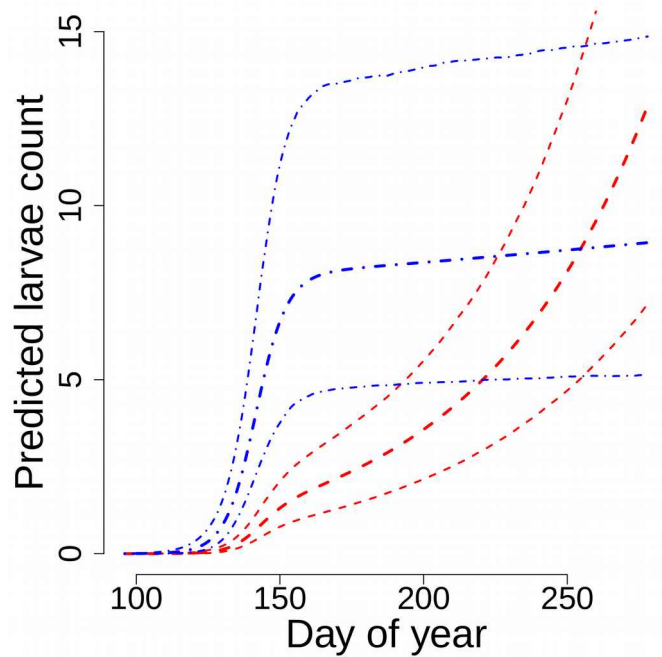
Trait	Distribution	Link	Predictor	Df	Deviance	Resid. DF	Resid. Dev	F	P-val		
Body length	Gaussian	Identity	Age	1	18100	1130	2651	17144	<0.0001		
			Age ²	1	468	1129	2183	443	<0.0001		
			Harvesting	1	130	1128	2053	123	<0.0001		
			Age x Harvesting	1	24	1127	2029	22	<0.0001		
			Age x Food	2	841	1125	1188	398	<0.0001		
			Age x Harvesting x Food	2	3	1123	1186	1	0.2650		
Maturation	Bernoulli	Logit	Age*	1	96	589	432	164	<0.0001		
			Length*	1	97	588	335	166	<0.0001		
			Harvesting	1	2	587	333	3	0.064		
			Food	2	3	585	329	3	0.0513		
			Age* x Harvesting	1	8	584	321	14	0.0002		
			Length* x Harvesting	1	1	583	320	2	0.1745		
			Age* x Food	2	12	581	309	10	<0.0001		
			Length* x Food	2	1	579	307	1	0.3263		
			Age* x Harvesting x Food	2	10	577	297	9	0.0002		
			Length* x Harvesting x Food	2	2	575	295	2	0.2027		

The structure of harvest-induced evolution



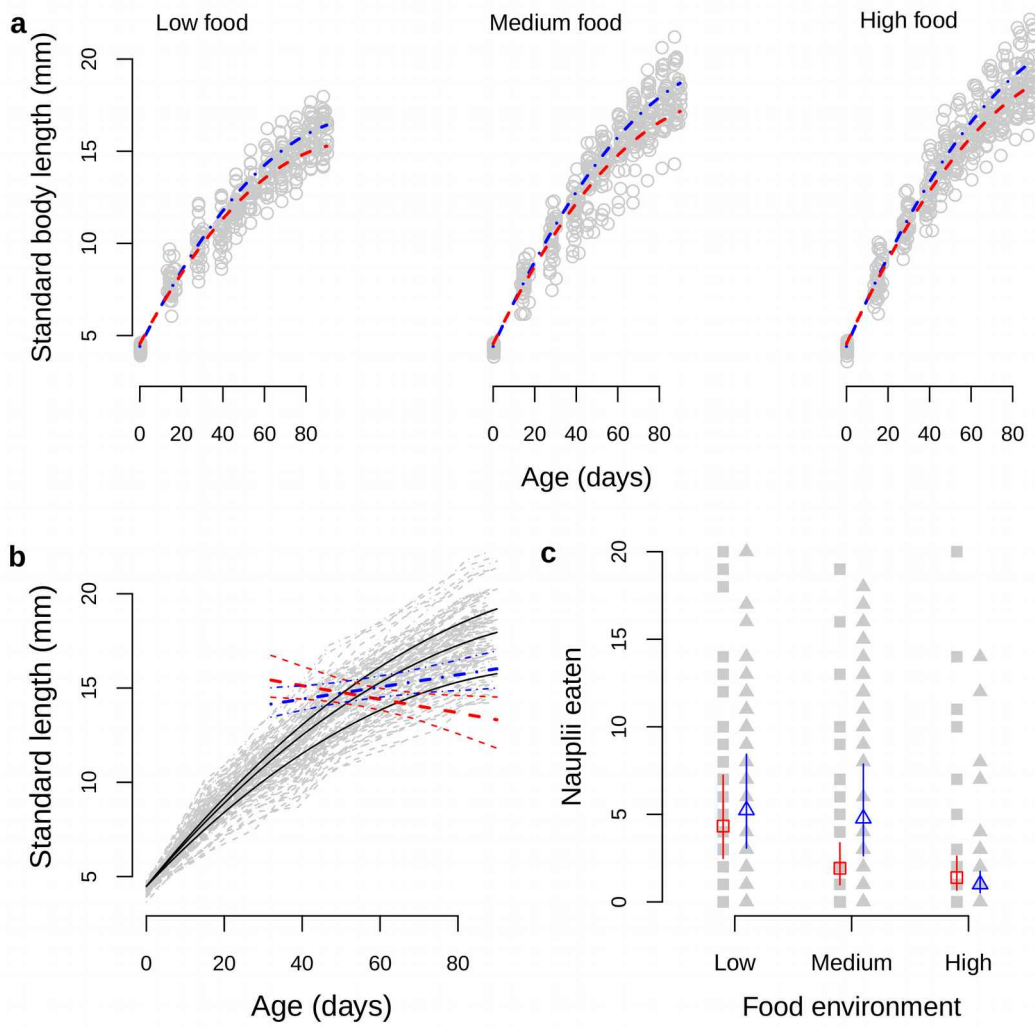
304 **Fig. 1. Direct and density-mediated harvest-selection in ponds. a: Size- and age-dependent**
305 **harvest selection.** Light grey bars represent raw standard length data in harvested populations.
306 Superimposed Gaussians represent mean MCMC estimates for the density of 0+ juveniles (short-
307 dashed curve) and 1+ and older adults (long-dashed curve) individuals. The magenta logistic curve
308 shows the mean relationship between exploitation rate by the fishery and standard body length. **b:**
309 **Stock-recruitment relationships.** Points show mean MCMC recruitment estimates with 95% credible
310 intervals for unharvested (blue triangles) and harvested (red squares) populations. Black curves show
311 year-specific Ricker functions fitted to mean estimates using maximum likelihood.

The structure of harvest-induced evolution



312 **Fig.2. Larvae count seasonal dynamics in ponds.** Thick curves represent mean MCMC estimates for
313 daily counts of newly-hatched larvae for unharvested (dot-dashed, blue curve) and harvested (dashed,
314 red curve) populations. Thin curves show 95% credible intervals around mean MCMC estimates.

The structure of harvest-induced evolution

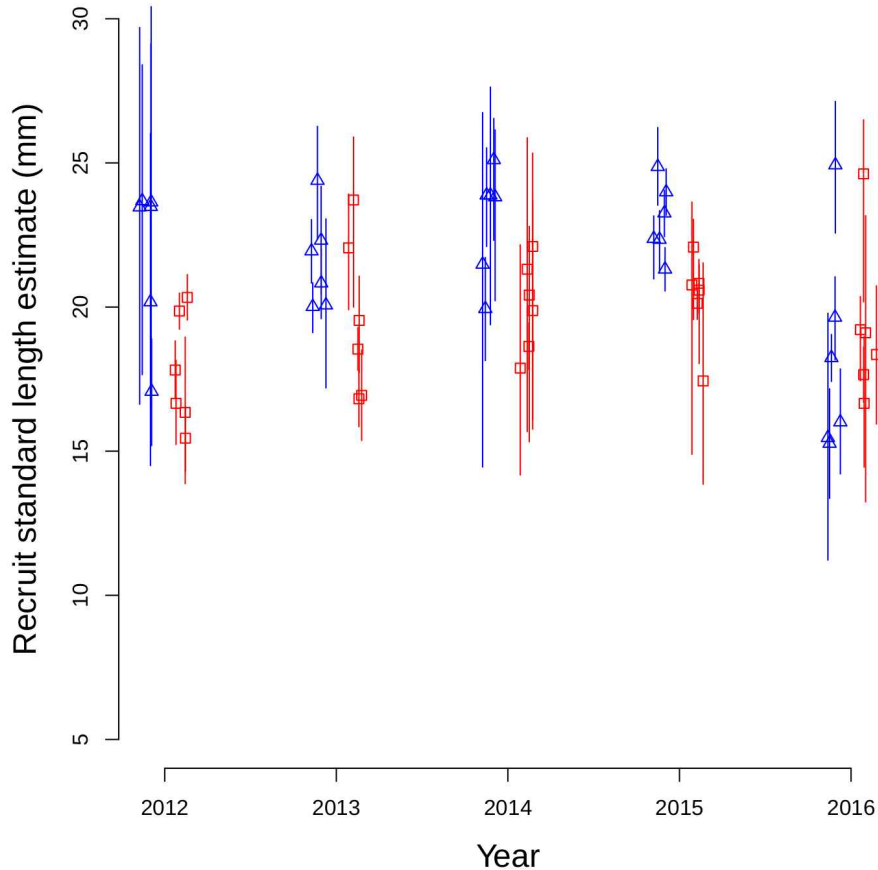


315 **Fig. 3. Individually-raised F₁ progeny in the laboratory. a: Mean growth trajectories.** MCMC
316 mean growth curves for individuals originating from unharvested (dot-dashed blue curves) and
317 harvested (dashed red curves) populations in a low-, medium- or high-food environments. Grey dots
318 show the raw data. **b: Probabilistic maturation reaction norms (PMRNs).** PMRNs show the
319 combination of age and lengths at which maturation probability equals 0.5. They account for the plastic
320 effect of growth on maturation, and a shift in PMRNs is thus suggestive of a non-plastic, evolutionary
321 change in maturation schedules (30, 31). Coloured lines show MCMC mean estimates with 95%

The structure of harvest-induced evolution

322 credible intervals for PMRNs of medaka originating from unharvested (dot-dashed blue line) and
323 harvested (dashed red line) populations. Thin grey curves in the background show raw growth
324 trajectories for medaka originating from unharvested (dot-dashed) and harvested (dashed) populations.
325 Solid black lines show the mean growth trajectories in a low-, medium- or high-food environment
326 (averaged across harvesting treatments). **c: Feeding rates.** Coloured, open points symbols show mean
327 MCMC estimates with 95% credible intervals for the number of prey eaten by medaka originating from
328 unharvested control (blue triangles) and harvested (red squares) populations and maintained in a low-,
329 medium- or high- food environment. Grey, filled symbols show the raw data.

The structure of harvest-induced evolution



330 **Fig. 4. Body length time series estimates for November 0+ recruits in pond medaka populations.**

331 Points show mean MCMC recruitment estimates with 95% credible intervals for unharvested (blue
332 triangles) and harvested (red squares) populations.

The structure of harvest-induced evolution

333 Supplementary Information for

334 **Density-dependent selection mediates harvest-induced evolution**

335 Alix Bouffet-Halle, Jacques Mériguet, David Carmignac, Simon Agostini, Alexis Millot,
336 Samuel Perret, Eric Motard, Beatriz Decenciere, Eric Edeline*

337 * Corresponding author: eric.edeline@inra.fr

338 **This PDF file includes:**

339 Supplementary methods: statistical analyses.
340 Table S1.

341 **Statistical analyses**

342 *Medaka aging in ponds*

343 Medaka juveniles are too small to be tagged and, unlike in Japan (1, 2), no winter check was deposited
344 in medaka otoliths in our experimental populations. We therefore relied on analysis of length-frequency
345 distributions to infer medaka age. We fitted a mixture of two Gaussian distributions to individual
346 standard body lengths Sdl_i :

$$347 Sdl_i \sim \sum_{j=1}^J \sum_{k=1}^K \pi_{j,k} N(\mu_{j,k}, \sigma_j^2) \quad (1a),$$
$$\mu_{2,k} \sim N(\mu_{H[k]}, \sigma^2)$$
$$\mu_{1,k} = \delta_k \mu_{2,k}$$
$$\delta_k \sim U(0,1)$$

The structure of harvest-induced evolution

348 where i indexes individuals ($n = 17908$), j indexes age groups (0+ vs. 1+ and older such that
349 $J = 2$), k indexes a sampling event, i.e., indexes one population in a particular year and month ($K = 109$ sampling events), N is the normal distribution, and U is the uniform distribution.
350 $H[k]$ indexes the harvest treatment (harvested vs. non harvested) associated with sampling event
351 k . $\pi_{j,k}$ is the proportion of age j individuals at each sampling event k such as for each
352 k :

354
$$\pi_j \geq 0, \sum_{j=1}^J \pi_j = 1 \quad (1b).$$

355 Indexes in line 1 in Eq. 1a show that our model estimated a mean standard body length separately for
356 each age group at each sampling event, while body length variance was assumed to vary only with age.
357 Line 2 in Eq. 1a shows that we assumed the mean standard body length of age 1+ and older medaka at
358 each sampling event $\mu_{2,k}$ to be a normally-distributed random variable with mean specific to each
359 harvest treatment, because harvesting was expected to restrict the maximum age and size of medaka.
360 Lines 3-4 in Eq. 1a show that mean standard body length of 0+ medaka at each sampling event $\mu_{1,k}$
361 was estimated as proportional to $\mu_{2,k}$ with a proportionality constant δ_k following a uniform
362 distribution U between 0 and 1. Model 1 provided us with MCMC age samples for each individual
363 fish in the dataset, allowing us to compute age-specific survival rates through the fishery.

364 We estimated temporal trends in mean standard body length of November 0+ recruits using a modified
365 version of model 1 that included a hierarchical regression:

The structure of harvest-induced evolution

$$\begin{aligned} Sdl_i &\sim \sum_{j=1}^J \sum_{k=1}^K \pi_{j,k} N(\mu_{j,k}, \sigma_j^2) \\ \mu_{2,k} &\sim N(\mu_{H[k]}, \sigma_2^2) \\ \mu_{1,k} &\sim N(\hat{\mu}_{1,k}, \sigma_1^2) \\ \hat{\mu}_{1,k} &= \alpha_{H[k]} + \beta_{H[k]} Year_k \end{aligned} \quad (1c)$$

366

367 where i indexes November-sampled fish ($n = 9688$ individuals, $K = 60$), $\alpha_{H[k]}$ and $\beta_{H[k]}$
368 are harvest treatment-specific temporal regression parameters, and $Year$ was scaled to 0 mean.
369 Other variables and subscripts are as described above.

370 *Fishery exploitation rate and selection in ponds*

371 We estimated the relationship between individual standard body length and probability to survive
372 through the fishery using a Bernoulli GLM with a logit link function:

$$\begin{aligned} y_i &\sim Bern(p_i) \\ \ln\left(\frac{p_i}{1-p_i}\right) &= \alpha_0 + \alpha_{j[i]} + (\beta_0 + \beta_{j[i]}) Sdl_i \quad (2), \\ \begin{pmatrix} \alpha_j \\ \beta_j \end{pmatrix} &\sim N\left(\begin{pmatrix} 0 \\ 0 \end{pmatrix}, \begin{pmatrix} \sigma_\alpha & \rho \sigma_\alpha \sigma_\beta \\ \rho \sigma_\beta \sigma_\alpha & \sigma_\beta \end{pmatrix}\right) \end{aligned}$$

373
374 where subscripts i and j index individuals ($n = 3970$) and groups, respectively, to which
375 individuals belong. There was $n = 6$ fished populations and $n = 5$ sampling years, yielding
376 $j = 1, 2, \dots, 30$ groups. Finally, $Bern$ is the Bernoulli distribution, and \ln is the natural
377 logarithm.

378 Eq. 2 indicates that we modelled the intercept and slope of the survival-mass relationship as normally-
379 varying among groups j , including a correlation parameter ρ between intercept and slope.

The structure of harvest-induced evolution

380 Parameter estimates α_0 and β_0 from Eq. 2 define a mean size-dependent survival function
381 $s(Sdl)=1/(1+\exp(-(α_0+β_0Sdl)))$ plotted in Fig. 1a.

382 *Stock-recruitment relationship in ponds*

383 Model (1) described above allowed us to estimate the number R_k of 0+ medaka (recruits) at each
384 November sampling event k ($n = 60$ November sampling events). We then visualized the strength of
385 negative density-dependence in pond medaka populations by plotting (Fig. 1b) Ricker (3) “stock-
386 recruitment” relationships between R_k and the number S_k of fish released in March (stock of
387 spawners):

388

$$\begin{aligned} R_k &\sim P(\lambda_k) \\ \ln(\lambda_k) &= \ln(S_k) + \alpha_{Year[k]} + \beta_{Year[k]} S_k \end{aligned} \quad (3),$$

389 where P is the Poisson distribution and $Year[k]$ indexes indicate that one Ricker curve was
390 fitted for each year from 2012 to 2016.

391 *Larvae counts*

392 Larvae counts L followed a zero-inflated negative binomial distribution and were modelled as (4):

393

$$\begin{aligned} L_i &\sim NB(\phi_i, r_i) \\ \phi_i &= \frac{r_i}{r_i + \lambda_i(1 - \theta_i)} \\ r_i &= \gamma_{H[i]} \\ \ln(\lambda_i) &= \alpha_{Year[i], Pond[i]} + \beta_{H[i]} + \delta_{H[i]} Day_i \\ \alpha_{Year[i], Pond[i]} &\sim N(0, \sigma_\alpha^2) \end{aligned} \quad (4a),$$

The structure of harvest-induced evolution

394 where subscript i indexes sampling events corresponding to a given observer in a given pond on a
395 given sampling day ($n = 2,004$ sampling events), NB is the negative binomial distribution with
396 success probability ϕ and number of failures r . Lines 4 and 5 in Eq. (4a) show that we modelled
397 positive (non-zero) counts λ as harvest treatment-specific linear regressions of the day of year
398 (scaled to 0 mean), with a normally-distributed random effect of the year and pond combination ($n = 36$
399 groups).

400 The θ latent variable for absence of larvae was modelled as a Bernoulli process having a linear
401 dependency on the day of year:

$$402 \quad \begin{aligned} \theta_i &\sim B(\psi_i) \\ \ln\left(\frac{\psi_i}{1-\psi_i}\right) &= \zeta + \omega Day_i \end{aligned} \quad (4b),$$

403 where B is the Bernoulli distribution with probability for absence of larvae ψ .

404 Line 3 in Eq. 4A shows that we allowed for r , which enters in the computation of the variance of
405 the distribution (4), to be different among the two harvest treatments H . Harvest treatment-specific
406 mean larvae count is given by $E(L_H) = \bar{\lambda}_H(1-\bar{\theta})$ and variance by
407 $var(L_H) = \bar{\lambda}_H(1-\bar{\theta})(\bar{\lambda}_H(1-\bar{\theta}) + \gamma_H)$, and we computed the dispersion index (4) in each harvest
408 treatment as $DI_H = E(L_H)/var(L_H)$ (Table S1).

409 *Somatic growth trajectories of F_1 progeny in the laboratory*

The structure of harvest-induced evolution

410 We estimated the effects of harvesting and food environments on medaka growth trajectories using a
411 second order polynomial regression of standard body length on age:

$$\begin{aligned} Sdl_i &\sim N(\mu_i, \sigma_i^2) \\ \mu_i &= \alpha_{P[i]} + \beta_{H[i]} + (\gamma_{H[i], F[i]} + \delta_{P[i]}) * Age_i + \eta Age_i^2 \\ \alpha_{P[i]} &\sim N(0, \sigma_\alpha^2) \\ \delta_{P[i]} &\sim N(0, \sigma_\delta^2) \\ \ln(\sigma_i^2) &= A_{H[i], F[i]} + B_{H[i], F[i]} Age_i \end{aligned} \quad (5),$$

413 where i indexes observations ($n = 1144$ observations from 104 individuals), $H[i]$ indexes the
414 harvest treatment associated with observation i , $H[i], F[i]$ indexes the interaction of harvest
415 treatment and food environment ($n = 2 * 3 = 6$ groups), and $P[i]$ indexes the parental breeding pair
416 associated with observation i ($n = 36$ pairs), treated as a normally-distributed random effect on both
417 size-at-hatch α and linear somatic growth rate δ (lines 3 and 4 in Eq. 5, respectively).

418 In this model, we assumed both linear somatic growth rate and the regression of (ln-transformed)
419 residuals variance on age to be different among harvest treatments and food environments (lines 2 and
420 5 in Eq. 5, respectively). In contrast, size-at-hatch $\beta_{H[i]}$ was allowed to vary only due to harvest
421 treatment because food environments were applied only starting from 15 dph.

422 *Probabilistic maturation reaction norms of F_1 progeny in the laboratory*

423 Probabilistic maturation reaction norms (PMRNs) describe the probability that an immature individual
424 at a given age and size will mature during a given interval of time (5). Provided that plasticity in the
425 maturation process is captured by growth trajectories, PMRNs separate the effects of evolution from

The structure of harvest-induced evolution

426 plasticity on maturation. PMRNs have been extensively used to explore genetic effects of exploitation
427 on the maturation process in wild populations (6, 7). Following the “direct estimation” method for
428 PMRNs (7), we fitted a Bernoulli model to individual medaka maturity (0 or 1) data y_i , truncated
429 so as to keep only the first maturity event for each individual:

$$y_i \sim B(M_i)$$

430 $\ln\left(\frac{M_i}{1-M_i}\right) = \alpha_{P[i]} + \beta_{H[i]} + \gamma_{H[i]} Age_i + \delta_{H[i]} Sdl_i \quad (6),$

$$\alpha_{P[i]} \sim N(0, \sigma_\alpha^2)$$

431 where M is maturity probability. Other subscripts or variables are as described above. Eq. 6 shows
432 that we allowed harvest-specific intercept and slopes of age and standard body length effects on
433 maturation probability. Harvest-specific PMRNs corresponding to length at 50% maturation probability
434 for each age in each treatment group H was then computed as $Sdl50_H = -(\beta_H + \gamma_H Age)/\delta_H$.

435 *Predatory behaviour of F_1 progeny in the laboratory*

436 Counts C_i of number of prey eaten by individual medaka followed a zero-inflated negative binomial
437 distribution and were modelled similarly as larvae counts in model 4 above:

$$C_i \sim NB(\phi_i, r_i)$$

438 $\phi_i = \frac{r_i}{r_i + \lambda_i(1 - \theta_i)}$ $(7a),$

$$r_i = \gamma_{H[i], F[i]}$$
$$\ln(\lambda_i) = \alpha_{I[i]} + \beta_{H[i], F[i]}$$
$$\alpha_{I[i]} \sim N(0, \sigma_\alpha^2)$$

The structure of harvest-induced evolution

439 where number of failures r and positive (non-zero) counts λ were both modelled as being
440 different among harvest treatments H in each food environment F , while $\alpha_{I[i]}$ was a
441 normally-distributed random individual effect on λ ($n = 3$ counts per individual). The θ latent
442 variable was modelled as:

$$\begin{aligned} \theta_i &\sim B(\psi_i) \\ 443 \quad \ln\left(\frac{\psi_i}{1-\psi_i}\right) &= \gamma + \delta_{I[i]} \quad (7b), \\ \delta_{I[i]} &\sim N(0, \sigma_\delta^2) \end{aligned}$$

444 where δ_I is a normally-distributed random individual effect.

445 *Analysis of deviance*

446 We tested for the overall statistical significance of harvest by food interaction on somatic growth and
447 maturation in the laboratory using analyses of deviance. Specifically, we fitted the following models:

$$\begin{aligned} 448 \quad Sdl_i &\sim N(\mu_i, \sigma_i^2) \\ \mu_i &= \alpha_{H[i]} + (\beta_{H[i]} + \gamma_{F[i]} + \delta_{H[i], F[i]}) Age_i + \zeta Age_i^2 \quad (8), \text{ and} \end{aligned}$$

$$\begin{aligned} 449 \quad y_i &\sim B(M_i) \\ \ln\left(\frac{M_i}{1-M_i}\right) &= \alpha_{H[i]} + \beta_{F[i]} + (\gamma_{H[i]} + \delta_{F[i]} + \zeta_{H[i], F[i]}) Age_i + (\eta_{H[i]} + \theta_{F[i]} + \iota_{H[i], F[i]}) Sdl_i \quad (9), \end{aligned}$$

450 where variables are as in models (5) and (6). We then used an F test to evaluate the significance of each
451 predictor separately (Table 1).

The structure of harvest-induced evolution

452 *Parameter estimation*

453 Models 3, 8 and 9 were fitted using maximum likelihood (glm function) in R 3.4.4 (8). Other models
454 were fitted by Markov chain Monte Carlo (MCMC) in JAGS 4.2.0 (9), through the jagsUI package
455 (10). To ease model convergence and avoid slope-intercept correlations, all numerical predictors were
456 scaled to zero mean. For each model, we ran three independent MCMC chains thinned at a period of 5
457 iterations until parameter convergence was reached, as assessed using the Gelman–Rubin statistic (11).

458 Parameter estimates for models 4-7 are provided in Table S1. Statistical significance of harvest- and
459 food-treatment effects reported in the main text was assessed from the posterior distributions of
460 parameter differences in a test equivalent to a bilateral t test. In these tests, the MCMC P-value was
461 twice the proportion of the posterior for which the sign was opposite to that of the mean posterior
462 value. For instance, in Eq. 4a the posterior differences $\beta_{H=1} - \beta_{H=0}$ and $\delta_{H=1} - \delta_{H=0}$ measure the
463 effect of harvest treatment (H = 0 for unharvested, H = 1 for harvested) on intercept and slope of day
464 effect for $\ln(\lambda)$, respectively.

465 Priors were chosen to be weakly informative. In model 1 we used a Dirichlet prior for the $\pi_{j,k}$ and
466 prevented label switching by assigning age class 0+ to fish shorter than 8 mm and age class 1+ and
467 older to fish longer than 35 mm (12).

468 We assessed goodness of fit of our models by using a Bayesian P-value (13). Briefly, we computed
469 residuals for the actual data as well as for synthetic data simulated from estimated model parameters
470 (i.e., residuals from fitting the model to “ideal” data). The Bayesian P-value is the proportion of

The structure of harvest-induced evolution

471 simulations in which ideal residuals are larger than true residuals. If the model fits the data well, the
472 Bayesian P-value is close to 0.5. Bayesian P values for our models ranged from 0.47 to 0.57 and were
473 on average 0.51, indicating excellent model fit to the data.

474 **References**

1. O. Terao, thesis, Tokyo (1985).
2. E. Edeline, O. Terao, K. Naruse, Empirical evidence for competition-driven semelparity in wild medaka. *Popul. Ecol.* **58**, 371–383 (2016).
3. W. E. Ricker, Stock and recruitment. *J. Fish. Res. Board Can.* **11**, 559–623 (1954).
4. I. Ntzoufras, *Bayesian modeling using WinBUGS* (Wiley, Hoboken (NJ), ed. 1, 2009).
5. M. Heino, U. Dieckmann, O. R. Godø, Measuring probabilistic reaction norms for age and size at maturation. *Evolution*. **56**, 669–678 (2002).
6. E. M. Olsen *et al.*, Maturation trends indicative of rapid evolution preceded the collapse of northern cod. *Nature*. **428**, 932–935 (2004).
7. M. Heino, U. Dieckmann, Detecting fisheries-induced life-history evolution: an overview of the reaction-norm approach. *Bull. Mar. Sci.* **83**, 69–93 (2008).
8. R Core Team, *R: a language and environment for statistical computing* (R Foundation for Statistical Computing, Vienna, Austria, 2018; <https://www.R-project.org/>).
9. M. Plummer, (Vienna, Austria, 2003).
10. K. Kellner, *jagsUI: a wrapper around “rjags” to streamline “JAGS” analyses* (2017; <https://CRAN.R-project.org/package=jagsUI>).
11. A. Gelman, D. B. Rubin, Inference from iterative simulation using multiple sequences. *Stat. Sci.*, 457–472 (1992).
12. H. Chung, E. Loken, J. L. Schafer, Difficulties in drawing inferences with finite-mixture models: a simple example with a simple solution. *Am. Stat.* **58**, 152–158 (2004).
13. A. Gelman, X. L. Meng, H. Stern, Posterior predictive assessment of model fitness via realized discrepancies. *Stat. Sin.* **6**, 733–807 (1996).

The structure of harvest-induced evolution

475 **Table S1. Structure and MCMC parameter estimates for models 4-7.** The MCMC P-value is twice
 476 the proportion of the posterior for which the sign was opposite to that of the mean posterior value. The
 477 MCMC P-values is not relevant for variance parameters that are constrained to be non-zero.

Model	Response	N	Distribution	Link	Effect	Mean estimate	SD of the estimate	MCMC P-value
4	Larvae count	2004	Bernoulli in ZINB	logit	Int.	-8.309	0.942	0.000
					Slope of day	-0.189	0.021	0.000
					Int. no-harvest	2.081	0.251	0.000
					Int. harvest	1.006	0.244	0.000
					Slope of day no-harvest	0.001	0.001	0.380
					Slope of day harvest	0.016	0.002	0.000
					Dispersion index no-harvest	8.702	2.089	
					Dispersion index harvest	2.417	0.359	
					SD of year by pond effect (random)	0.998	0.137	
5	Standard body length	1144	Gaussian	Identity	Int. no-harvest	4.410	0.106	0.000
					Int. harvest	4.548	0.099	0.000
					Slope of age no-harvest low food	0.224	0.005	0.000
					Slope of age harvest low food	0.210	0.005	0.000
					Slope of age no-harvest medium food	0.250	0.005	0.000
					Slope of age harvest medium food	0.231	0.005	0.000
					Slope of age no-harvest high food	0.263	0.005	0.000
					Slope of age harvest high food	0.248	0.004	0.000
					Slope of age squared	-0.001	0.000	0.000
					Int. residual variance no-harvest low food	-0.021	0.157	0.854
					Int. residual variance harvest low food	-0.549	0.127	0.001
					Int. residual variance no-harvest medium food	-0.597	0.155	0.002
					Int. residual variance harvest medium food	-0.384	0.130	0.004
					Int. residual variance no-harvest high food	-0.520	0.129	0.000
					Int. residual variance harvest high food	-0.295	0.145	0.043
					Slope of age residual variance no-harvest low food	-0.005	0.003	0.079
					Slope of age residual variance harvest low food	0.011	0.002	0.000
					Slope of age residual variance no-harvest medium f	0.000	0.004	0.923
					Slope of age residual variance harvest medium food	0.010	0.002	0.000
					Slope of age residual variance no-harvest high food	0.011	0.002	0.000
					Slope of age residual variance harvest high food	-0.011	0.003	0.001
					SD of parental pair effect on int. (random)			
					SD of parental pair on slope of Age effect (random)			
6	Maturation probability	591	Bernoulli	logit	Int. no-harvest	-4.138	0.698	0.000
					Int. harvest	-4.762	0.771	0.000
					Slope of age no-harvest	-0.054	0.025	0.020
					Slope of age harvest	0.055	0.024	0.025
					Slope of length no-harvest	1.662	0.286	0.000
					Slope of length harvest	1.521	0.271	0.000
					SD of parental pair effect on int. (random)	1.470	0.356	
7	Prey count	311	Negative binomial in ZINB	logit	Int.	-1.960	0.541	0.000
					SD of individual effect (random)	0.903	0.534	
					Int. no-harvest, low food	2.035	0.208	0.000
					Int. harvest, low food	1.848	0.231	0.000
					Int. no-harvest, medium food	1.928	0.245	0.000
					Int. harvest, medium food	0.986	0.286	0.001
					Int. no-harvest, high food	0.357	0.270	0.188
					Int. harvest, high food	0.672	0.309	0.025
					Dispersion index no-harvest, low food	2.388	0.722	
					Dispersion index harvest, low food	5.994	2.141	
					Dispersion index no-harvest, medium food	6.509	3.857	
					Dispersion index harvest, medium food	5.012	2.357	
					Dispersion index no-harvest, high food	2.033	0.710	
					Dispersion index harvest, high food	5.708	2.642	
					SD of individual effect (random)	0.681	0.136	